Russian Journal of Earth Sciences

Spatial and Temporal Variability of Chlorophyll-*a* and the Modeling of High-Productivity Zones Based on Environmental Parameters: a Case Study for the European Arctic Corridor

Sofia Kuzmina[*,1,2], **Polina Lobanova**[1], **and Svetlana Chepikova**[3]

[1]Saint Petersburg State University, Saint Petersburg, Russia
[2]Alfred-Wegener-Institut Helmholtz-Zentrum für Polar- und Meeresforschung, Bremerhaven, Germany
[3]State Hydrological Institute, St. Petersburg, Russia
* **Correspondence to:** Sofia Kuzmina, so.k.kuzmina@gmail.com

Abstract: Over the past 20 years, increasing temperature and receding ice-cover have led to changes in the Arctic ecosystem. Our study aims to create models that predict the position of high chlorophyll-*a* concentration (Chl-*a*) zones in the European Arctic Corridor (the Barents, Norwegian and Greenland Seas) to monitor these changes. Firstly, we use remotely sensed data to assess spatial and temporal changes in correlation between Chl-*a* and environmental parameters that could influence Chl-*a* in the region – Photosynthetically Active Radiation (PAR), Sea Surface Temperature (SST), Mixed Layer Depth (MLD) and Sea Surface Salinity (SSS) – over the 2010–2019 time period. We found significant correlation ($|r|$ = 0.6–0.8) between Chl-*a* and PAR and SST, and medium correlation ($|r|$ = 0.4–0.6) between Chl-*a* and SSS and MLD, correlation was highest during spring periods. Then, using a Random Forest Machine Learning algorithm in the Classifier modification, we created models for each sea to predict the position of high-productivity zones (Chl-*a* > 1 mg m^{-3}) using environmental parameters. Our results suggested that Chl-*a* variability in the European Arctic Corridor is mostly determined by PAR (28–32% of Chl-*a* class variability), SST (25–29%), and SSS (26–31%); MLD played a lesser role (12–17%). According to validation, all the models showed high performance scores (F1-score = 66–95%) and slightly underestimated the total area of high productivity.

Keywords: chlorophyll-*a*, ocean productivity, Arctic Ocean, modeling, ocean colour, remote sensing, Barents Sea, Norwegian Sea, Greenland Sea.

Citation: Kuzmina, S., P. Lobanova, S. Chepikova (2025), Spatial and Temporal Variability of Chlorophyll-*a* and the Modeling of High-Productivity Zones Based on Environmental Parameters: a Case Study for the European Arctic Corridor, *Russian Journal of Earth Sciences*, 25, ES1010, EDN: SDYCMN, https://doi.org/10.2205/2025es000952

Research Article

Received: 5 March 2024
Accepted: 15 October 2024
Published: 10 March 2025

1. Introduction

The European Arctic Corridor, or EAC, (Figure 1) accounts for about 50% of the total primary production of the Arctic, making it a highly productive region [*Oziel et al.*, 2020, 2022; *Sakshaug et al.*, 2009; *Siegel et al.*, 2002]. This is due to several factors. Firstly, two types of water masses meet in the area: warm and salty Atlantic waters, and cold and relatively fresh Arctic waters that form frontal zones characterized by high productivity [*Hansen et al.*, 1990; *Longhurst*, 2007; *Makarevich et al.*, 2022; *Qu and Gabric*, 2022]. Secondly, energy associated with the North Atlantic Current contributes to the breakdown of stratification in summer, and therefore, a flux of nutrients into the surface layer necessary for phytoplankton growth [*Sakshaug et al.*, 2009]. Finally, the area is partially covered in ice, which adds to the formation of phytoplankton blooms specific to polar latitudes, including ice-edge blooms that contribute significantly to the overall productivity of the region [*Anderson*, 1986; *Borstad and Gower*, 1984].

Over the past 20 years, productivity of polar seas has been changing due to the instability of the climate, which is the most pronounced in the Arctic [*Arrigo and van Dijken*, 2015; *Oziel et al.*, 2022; *Wassmann et al.*, 2010]. Rising temperature and reduced sea ice cover add to the changes in overall conditions contributing to a phytoplankton bloom: higher overall temperature and earlier warming of the water column could lead to an earlier bloom onset; lessening sea-ice cover could lead to a greater surface area available for phytoplankton to bloom [*Oziel et al.*, 2020]. An earlier phytoplankton bloom with a larger surface area could lead to a higher overall productivity for the region [*Lewis et al.*, 2020]. To assess and monitor these changes accurately, it is necessary to have an extensive database of ocean productivity. The biggest problem in studying ocean productivity in the ocean, and in the Arctic especially, is the lack of in situ data needed for a statistically significant analysis of its spatial and temporal variability: a possible solution is using remotely sensed data to study the productivity of the Arctic [*Lee et al.*, 2015a].

Ocean productivity can be estimated via its relationship with chlorophyll-*a* concentration (Chl-*a*), since organic matter production is a result of photosynthesis, which utilizes chlorophyll pigments (mainly Chl-*a*) [*Delafontaine and Peters*, 1986; *Lee et al.*, 2015a; *Ryther and Yentsch*, 1957]. The study of ocean productivity based on satellite data provides the basis for modeling PP for the Arctic as a whole: once one has determined the contribution of multiple environmental factors to Chl-*a* variability in the surface layer, one would be able to develop models for assessing Arctic waters' productivity – in our case, the productivity of EAC [*Kuzmina et al.*, 2022, 2023; *Lee et al.*, 2015a; *Martyanov et al.*, 2018; *Oliver et al.*, 2018; *Skogen et al.*, 1995; *Slagstad and Støle-Hansen*, 1991; *Vernet et al.*, 2021; *Wassmann et al.*, 2006].

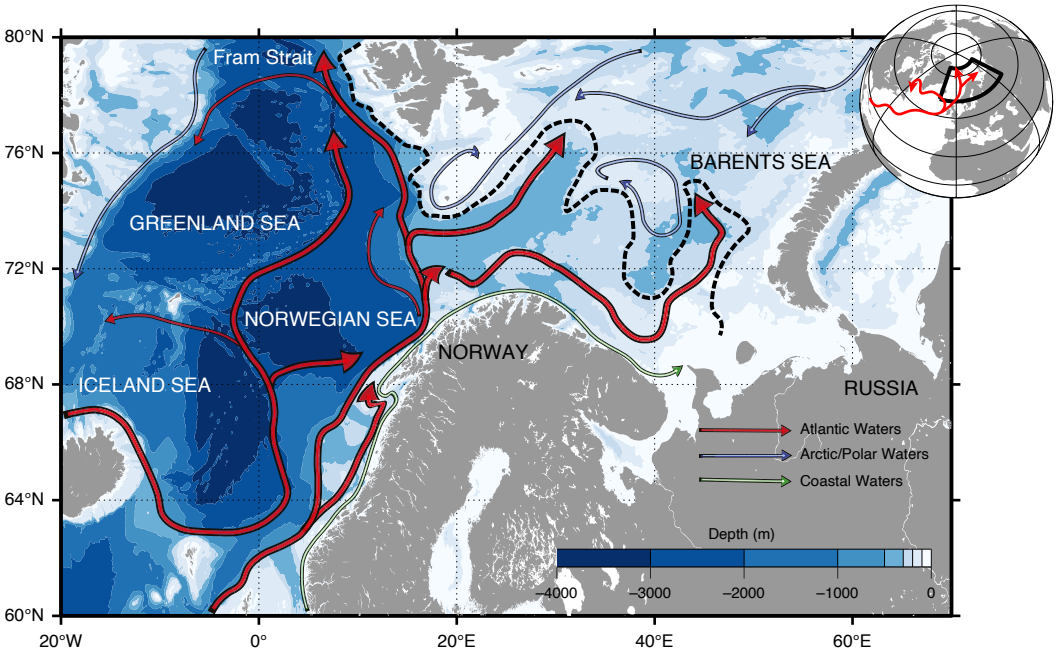

Figure 1. Map of the European Arctic Corridor. Surface currents are: polar waters in blue, coastal waters in green, Atlantic waters – in red. Dashed black line is the Barents Sea polar front. From [*Oziel et al.*, 2020].

Defining the term "ocean productivity" is divided into two schools of thought: viewing productivity (1) as a process occurring at a certain rate in a single volume – i.e., the rate of synthesis of organic matter, or photosynthesis [*Behrenfeld and Falkowski*, 1997; *Platt and Sathyendranath*, 1988], and (2) as an amount of substance (for example, carbon or Chl-*a* pigment) formed in a single volume per unit of time – i.e., the amount of photosynthetic products produced in a single time unit [*Behrenfeld et al.*, 2005; *Carr et al.*, 2006; *Falkowski et al.*, 1998; *Nielsen*, 1963; *Riley*, 1940].

Following the second definition, a higher Chl-*a* would suggest a higher value of ocean productivity in an area. While we acknowledge that there is a complex and non-linear connection between Chl-*a* and ocean productivity, we believe that Chl-*a* is still a good indicator of overall ocean productivity on a monthly scale [*Bode et al.*, 2011].

Therefore, in this study we assess the productivity of the EAC by assessing the position and overall total area of *high-productivity zones* (HPZs) in the EAC. We define these HPZs using a threshold value of Chl-*a* in a grid cell (4 × 4 km) – greater than 1 mg m^{-3} [*Balch*, 1992; *Carr*, 2001], – and zones with Chl-*a* below that threshold value are assumed to be *low-productivity zones* (LPZs) [*Lee et al.*, 2015b].

It is worth noting that in this case we model only part of the region's productivity, mostly so for the Barents Sea [*Kondrik et al.*, 2017]. This is the part that is mostly attributed to algae like diatoms and dinoflagellates, i.e., algae that do not have a calcium skeleton, algae that we observe using ocean color Chl-*a* images. The presence of coccolithophores – another very abundant species for the EAC – is reflected in other parts of the color spectra (with wavelengths not used in this study [*Balch et al.*, 1991]), and their productivity cannot be assessed through standard ocean color products. It means that in this study, the productivity of the region can be estimated to be somewhat less than in situ productivity. One must also take into account the fact that coccolithophore presence affects the optical properties of the waters: during a coccolithophore bloom, higher $R_{rs}(\lambda)$ in the blue and green areas of the spectrum have been observed in the Baltic, North and Celtic Seas, although usually the accuracy of ocean color products is not degraded significantly [*Cazzaniga et al.*, 2021].

Because autotrophic organisms' productivity is determined by photosynthesis, occurring via the pigment Chl-*a*, it is influenced by those environmental factors that contribute to the maximum rate of photosynthesis and phytoplankton growth. These are, in order of highest contribution: light [*Morel*, 1978; *Odum*, 1971], nutrients (which enter the upper ocean layers as a result of upwelling, horizontal advection (surface currents, polar fronts), with river runoff, ice sheet melt, and precipitation [*Chandler et al.*, 2015; *Sverdrup*, 1953]), and sea surface temperature (SST) [*Talling*, 1957; *Teira et al.*, 2005].

The study region is characterized by two phytoplankton blooms: in spring and autumn [*Ardyna et al.*, 2014; *Kahru et al.*, 2011]. In the Greenland and Norwegian Seas, the bloom occurs later than in the Barents Sea (June and May, respectively); the autumnal bloom is usually more intense than the spring one, and this intensity is ever-increasing due to overall climate changes in the Arctic [*Ardyna et al.*, 2014; *Lewis et al.*, 2020; *Longhurst*, 2007; *Vernet et al.*, 2021]. In each sea, a spring bloom peak occurs firstly in the southern part of the sea, gradually moving northward [*Qu and Gabric*, 2022]. Maximum Chl-*a* is observed in the southern parts of the seas, near ice edges [*Perrette et al.*, 2011], on the shelf, as well as in the frontal regions [*Reigstad et al.*, 2002]. Chl-*a* is often higher in the Barents and Norwegian Seas than in the Greenland Sea [*Qu and Gabric*, 2022]; however, the duration of the spring bloom in the Norwegian Sea is shorter [*Børsheim et al.*, 2014].

The purpose of this work is to identify environmental factors that determine Chl-*a* in EAC waters (case study for the Barents, Norwegian, and Greenland Seas), as well as to create and validate models for the position of HPZs using the Random Forest machine learning algorithm in the Classifier modification (RF). This work has, as far as the authors are aware, for the first time, used RF to predict the position of HPZs and LPZs (as Chl-*a* classes) in the European Arctic Corridor and identify the remotely-sensed factors that influence it.

2. Materials and Methods

The following satellite and reanalysis data were used in the study: 1) ocean color data from the Ocean Colour Climate Change Initiative database, version 5 (https://www.oceancolour.org) – chlorophyll-*a* concentration (Chl-*a*, mg m^{-3}) and euphotic layer depth (Zeu, m), monthly data in 4 × 4 km pixels; the latter was calculated as a function of a diffuse attenuation coefficient at 490 nm (K_d490) described in [*Lobanova*, 2017]; 2) mixed layer depth (MLD, m) calculated using a method by Dukhovsky D.S. presented in [*Bashmachnikov*

et al., 2018] on the basis of vertical density profiles obtained from temperature and salinity data from the EN4 Hadley Center and ARMOR data bases, monthly data in 4 × 4 km pixels; 3) sea surface salinity (SSS, psu) from the Microwave Imaging Radiometer with Aperture Synthesis (MIRAS) satellite Soil Moisture and Ocean Salinity (SMOS) from the European database Space Agency (ESA) (https://earth.esa.int), monthly data in 25 × 25 km pixels; 4) sea surface temperature (SST, °C) from NASA's Physical Oceanography Distributed Active Archive Center MUR SST database (https://podaac.jpl.nasa.gov/MEaSUREs-MUR), daily data in 1 × 1 km pixels; 5) photosynthetically active radiation (PAR, $\mathrm{E\,m^2\,day^{-1}}$) from the MODIS-Aqua spectroradiometer from NASA's Ocean Biology Processing Group database (https://oceancolor.gsfc.nasa.gov), monthly data in 4 × 4 km pixels.

All data were interpolated to a grid with a spatial resolution of 4 × 4 km using the 2D linear interpolation available in MATLAB, and averaged monthly for the period from 2010 to 2019. This was done to eliminate gaps in data caused by atmospheric interference such as, for example, cloud cover for ocean color data.

To estimate the connection between Chl-*a* and environmental parameters we used Pearson's correlation coefficient:

$r(A,B) = \frac{1}{N-1}\sum_{i=1}^{N}\left(\frac{A_i-\mu_A}{\sigma_A}\right)\cdot\left(\frac{B_i-\mu_B}{\sigma_B}\right)$, where $\mu_{A/B}$ and $\sigma_{A/B}$ are the mean and standard deviation of A/B.

In each 4 × 4 km pixel we created vectors with a value of the parameter for each month in the time period from 2010 to 2019 for all available data and calculated the correlation coefficient between the Chl-*a* vector and the environmental parameter vectors. For each pixel we had between 20 to 30 available data points, 5–20 for autumnal data, and the data availability was the most limited in the northernmost parts of the region, where sea ice cover and clouds prevented data access the most (see Appendix A, Figure A1).

To predict the position of HPZ, for the first time a Random Forest machine learning algorithm was used in the Classifier modification, which has already proven itself to be a useful research tool in different environmental studies [*Cutler et al.*, 2007; *Kuzmina et al.*, 2023; *Rivero-Calle et al.*, 2015].

Random Forest Classifier is a machine learning algorithm that uses decision trees to classify data. The advantages of using this algorithm in particular are that it 1) allows for non-linear connections between data points, 2) allows for spatially and temporally non-continuous datasets and 3) is resistant to overfitting.

When modeling, to define the position of high- and low-productivity zones all Chl-*a* values were divided into two data sets distinguishing these zones, resulting in two classes: the HPZ class and the LPZ class, the positions of which were later predicted by the proposed models. The allocation of classes was determined by a threshold value for Chl-*a* of $1\ \mathrm{mg\,m^{-3}}$ [*Balch*, 1992].

The resulting data sets were divided into training and test data sets using a ratio conventional for machine learning of 2:1 respectively for each sea. For the second validation set, we used all available data except year 2019 as a training set to maximize the accuracy of our models' performance by maximizing the amount of training data available to the algorithm [*Joseph*, 2022; *Nguyen et al.*, 2021].

Three models were developed: one for each sea in the EAC.

Based on our results, we obtained quantitative estimates (precision, recall, and F1-score) of the quality of the models:

$$\text{Precision} = TP/(TP+FP)\cdot 100\%,$$

$$\text{Recall} = TP/(TP+FN)\cdot 100\%,$$

$$\text{F1-score} = (2\cdot\text{Precision}\cdot\text{Recall})/(\text{Precision}+\text{Recall})\cdot 100\%,$$

where TP is true positive (correctly predicted class), FP – false positive (incorrectly predicted class in terms of overestimation, i.e., detection of a class where there was not one

in the test data), and *FN* – false negative values (incorrectly predicted class in terms of underestimation, i.e., non-detection of a class where there was one in the test data), F1-score – the weighted average between precision and recall. Resulting metrics describe the proportion of correctly predicted cases: thus, 100% is the best indicator for each metric, 0% – the worst.

3. Results

3.1. Relationship Between Chlorophyll-a Concentration and Environmental Parameters

To estimate the relationship between Chl-*a* and environmental factors we analyzed spatial and temporal variability of the correlation coefficients between the parameters for the entire study period (Figures 2–3). The closest relationship between the parameters can be seen in spring: at this time, the correlation between Chl-*a* and PAR is positive, between Chl-*a* and SST is positive in open waters, negative – in coastal waters ($|r| > 0.4$). Following high correlation between Chl-*a* and SST, dynamically active Atlantic waters can be traced; as their effect weakens when going further northward, correlation decreases.

In summer, correlation between Chl-*a* and SST is negative in the Norwegian and Greenland Seas, and positive in the southern and central part of the Barents Sea ($|r| = 0.4$–0.6). The reverse is typical for Chl-*a* and PAR: the correlation is positive in the Norwegian and Greenland Seas and the northern part of the Barents Sea, negative – in the coastal part of the Barents Sea ($|r| = 0.6$–0.8).

During autumn, spatial variability of correlation between Chl-*a* and environmental parameters becomes more non-linear: correlation between Chl-*a* and SST in open waters of the Barents and eastern Greenland Seas is positive, but lower than in spring. In coastal waters, the Norwegian Sea and the western part of the Greenland Sea correlation is reversed. The correlation between Chl-*a* and PAR is mostly negative in contrast to the spring period, and less pronounced.

The correlations between Chl-*a* and SSS, Chl-*a* and MLD are the most homogenous in spring (Figure 3): correlation between Chl-*a* and SSS is positive, between Chl-*a* and MLD – negative ($|r| = 0.4$–0.6).

In summer, the correlation between Chl-*a* and these two parameters is mostly low ($|r| < 0.2$), positive moderately high correlation between Chl-*a* and SSS is observed in the east of the Barents Sea, and between Chl-*a* and MLD – in the Greenland Sea. For SSS, negative moderately high correlation is also observed near the coast and in the east of the Greenland and Norwegian Seas, while an area characterized by positive correlation shifts to the west towards a mixing zone of the Norwegian (warm) and the East Greenland (cold) currents.

In autumn, the correlation distribution between the parameters appears to be the most non-linear. For Chl-*a* and SSS, in the central part of the Barents and Norwegian Seas, positive correlation is observed ($r > 0.4$), in the Greenland Sea and in the north of the Barents and Norwegian Seas there is negative correlation ($|r| = 0.4$–0.6). For Chl-*a* and MLD, the areas of positive correlation are: the southern part of the Barents Sea, a border between the Barents and Norwegian Seas, and the Greenland Sea frontal zones, where active mixing occurs; in other areas correlation is predominantly negative.

3.2. Development and validation of the models

Using the Random Forest machine learning algorithm, we developed models to predict the position of high- and low-productivity zones in the study area. Model Quality Metrics (MQMs) exceed 90% for each sea for the initial test sample (Table 1). The models for the Greenland and Barents Seas show slightly higher MQMs (by 3–5%) than the model for the Norwegian Sea.

In the preliminary testing, we also considered Zeu as a predictor. However, this resulted in the contribution of Zeu to the variability of Chl-*a* classes being more than 80% of all predictors' (Zeu, PAR, SST, SSS, MLD). Almost 90% of Chl-*a* class' variability was accounted for by Zeu and PAR (81–82% and 6–8% respectively), and SST, SSS and MLD accounted for between 3 to 5% of variability. We made the decision to then remove Zeu as a predictor, as, firstly, the Zeu data is available with the same discrepancy as Chl-*a*

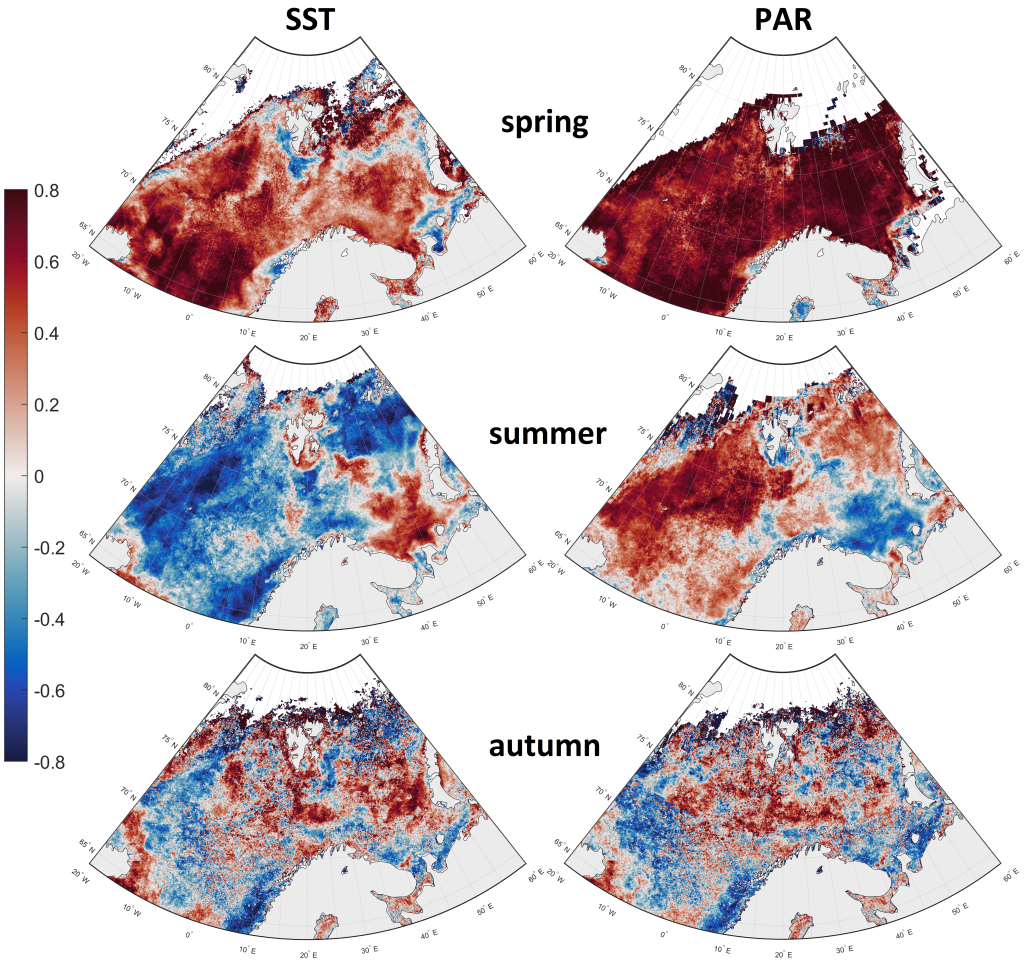

Figure 2. Spatial and temporal variability of a correlation coefficient between chlorophyll-*a* concentration (Chl-*a*, mg m^{-3}) and environmental parameters: sea surface temperature (SST, °C), and photosynthetically active radiation (PAR, E m^2 day^{-1}) in 2010–2019. The correlation coefficient is grouped and calculated by seasons. All correlation coefficients have a p-value ≤ 0.05.

data – therefore, our models would not expand our understanding of HPZs' positions in high cloud-cover, low-light areas. Moreover, we came to the conclusion that this would be a falsely strong connection, seeing as Zeu was calculated through K_d490 – a parameter that accounts for the amount of suspended particles in the water. Seeing as most of the study area is type I waters – where most suspended matter is phytoplankton – we believe that this connection is mostly artificial [*Morel and Prieur*, 1977]. Therefore, we have made the decision to remove Zeu as a predictor to better understand how environmental factors – PAR, SST, SSS and MLD, – account for Chl-*a* variability.

Based on the results of the models, the contribution of the environmental parameters to the variability of the position of high-productivity zones (i.e., Chl-*a* classes) in the area was estimated (Table 1). Here, the greatest contribution to the spatial and temporal variability of HPZs was made by PAR, SSS and SST: for PAR, this contribution is 28–32%, depending on the sea, for SSS it is 26–31%, and for SST it is 25–29%, however, MLD accounts for only 12–17% of the variability.

To further evaluate the models' performance, we validated them for the year 2019, which is the last year available for the analysis. For this, the training set consisted of all available data except for 2019, and the test one was the 11 available months of year 2019 (January – November). MQMs for this data set retained high values, although decreased slightly: precision: 67–71%, recall: 66–68%, F1-score: 66–68%. This is the dataset that shall now be discussed in further detail.

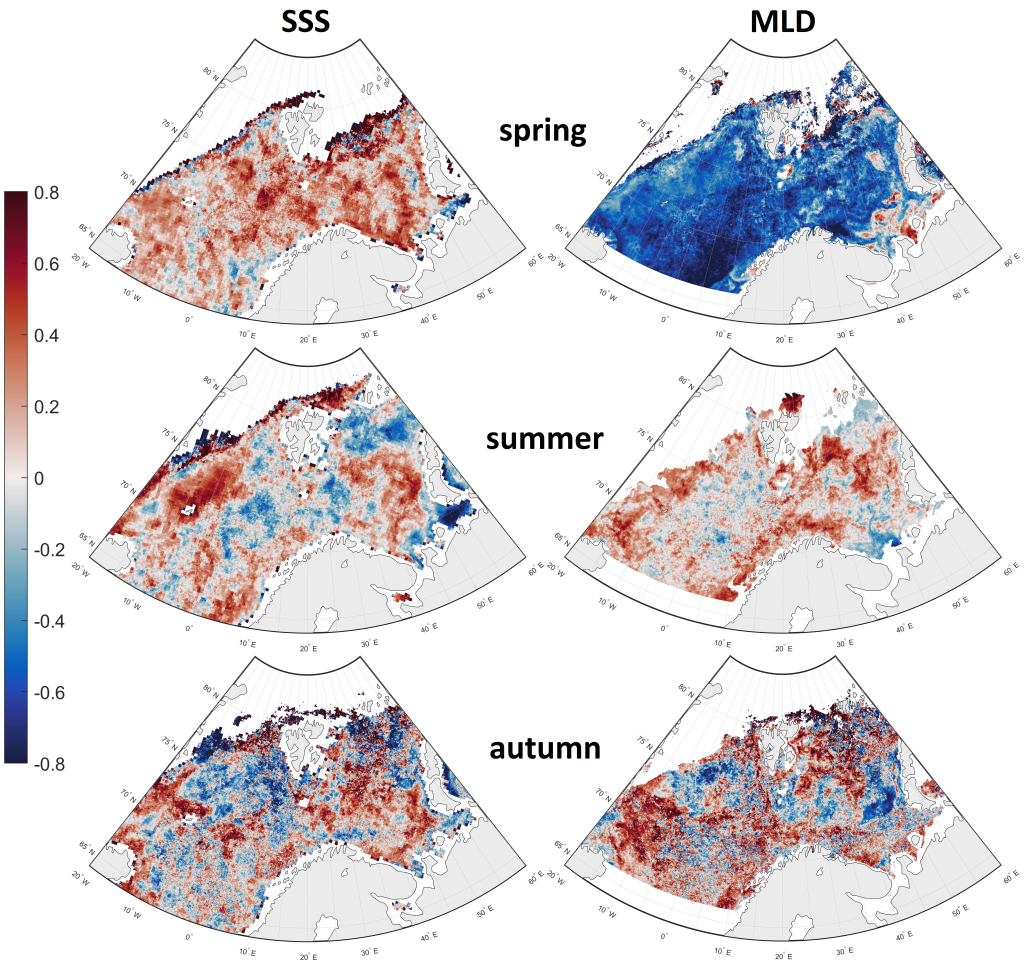

Figure 3. Spatial and temporal variability of a correlation coefficient between chlorophyll-*a* concentration (Chl-*a*, mg m^{-3}) and environmental parameters: sea surface salinity (SSS, psu) and mixed layer depth (MLD, m) in 2010–2019. The correlation coefficient is grouped and calculated by seasons. All correlation coefficients have a p-value ≤ 0.05.

Based on the analysis of the models, all three quite accurately represent the general nature of both temporal (Figure 4) and spatial (Figure 5) variability of the distribution of high- and low-productivity zones. The model for the Greenland Sea achieves this best in terms of overall performance (highest MQMs), seeing as it almost always correctly shows the position of HPZs, however, it lacks in quantitive assessment, as it underestimates total HPZ area during an autumn bloom. The model for the Norwegian Sea generally correctly predicts the position of HPZs, but underestimates the total area of HPZs, especially during spring and autumn blooms. The Barents Sea model does not always correctly predict HPZ position, however it predicts the total area of HPZs during a spring bloom (March – June) the best out of the three models and only during the autumn bloom does it underestimate it.

As can be seen from Figure 5, the most accurate results for the models are characteristic for months with lower Chl-*a*. For the Norwegian and Greenland Seas, the greatest bias both in the extension of HPZs and in their position occurs during a spring bloom (May – June); for the Barents Sea, the greatest bias in predicting the total HPZ area is characteristic of the autumn bloom (September – October); in predicting the position of HPZs – for the spring bloom.

Table 1. Contribution (in %) of environmental parameters to the variability of chlorophyll-*a* concentration classes in the seas. Here PAR is photosynthetically active radiation, SST is sea surface temperature, MLD is mixed layer depth. To assess the accuracy of the models, the following model quality metrics were used: precision, recall, and F1-score. Metrics in brackets refer to the metrics for two classes – LPZ and HPZ, metrics in bold refer to a mean metric between the two classes

Parameter	Barents Sea	Norwegian Sea	Greenland Sea
PAR	29%	28%	32%
SST	28%	29%	25%
SSS	31%	26%	28%
MLD	12%	17%	14%
Model Quality Metrics			
Precision	**0.96** (0.95; 0.97)	**0.93** (0.95; 0.90)	**0.96** (0.97; 0.95)
Recall	**0.96** (0.93; 0.98)	**0.91** (0.97; 0.86)	**0.95** (0.97; 0.93)
F1-score	**0.95** (0.94; 0.97)	**0.92** (0.96; 0.88)	**0.95** (0.97; 0.94)
Data set size in 4 × 4 km pixels, training/test data	1,774,134/887,067	613,026/306,513	862,802/431,401

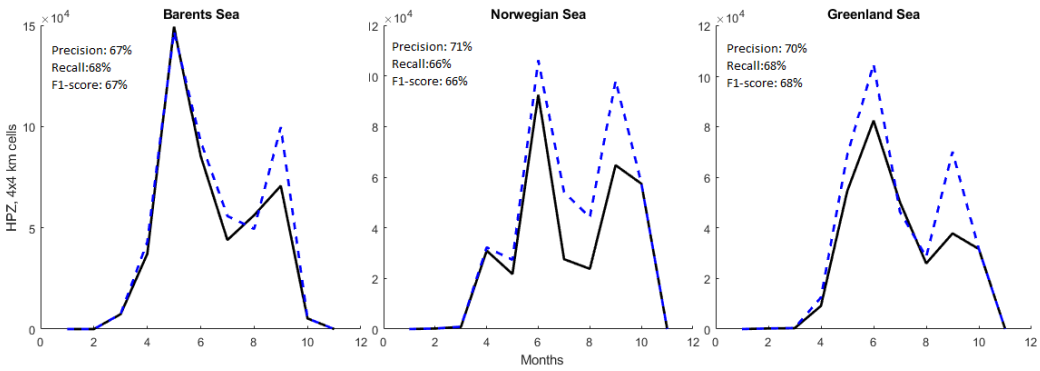

Figure 4. Validation results for the proposed models. Comparison of the estimated and remotely sensed total area of high-productivity zones (total sum of high-productivity cells in the region) based on chlorophyll-*a* concentration in 2019. Solid black line is satellite data (test set), dotted blue line is data estimated by the models for the same period.

4. Discussion

4.1. Sverdrup's Critical Depth Hypothesis

According to Sverdrup's theory, a bloom can begin when MLD becomes shallower in the late spring – early summer period, when most of the phytoplankton concentrate inside the euphotic layer above the critical depth [*Sverdrup*, 1953]. The theory has been confirmed many times both by Sverdrup himself and by other researchers for different water bodies [*Brody and Lozier*, 2015; *Delafontaine and Peters*, 1986; *Sathyendranath et al.*, 2015; *Siegel et al.*, 2002]. However, in recent years, more and more researches have argued against it [*Behrenfeld*, 2010; *Chiswell*, 2011; *Fischer et al.*, 2014; *Lewandowska et al.*, 2015]. The theory describes an idealized, uniformly mixed layer; it does not take into account convection rate and turbulent flows within the layer, and it does not consider changes in composition in auto- and heterotrophic communities; a phytoplankton spring bloom often does not coincide with the formation of steady stratification, but begins somewhat earlier [*Behrenfeld*, 2010]. Despite the criticism of the theory, according to the results of our study (the relationship between Chl-*a* and MLD, see Figure 3), this hypothesis could be confirmed when describing the general annual cycle of phytoplankton growth: the correlation between Chl-*a* and MLD is negative in spring, when at the beginning of the

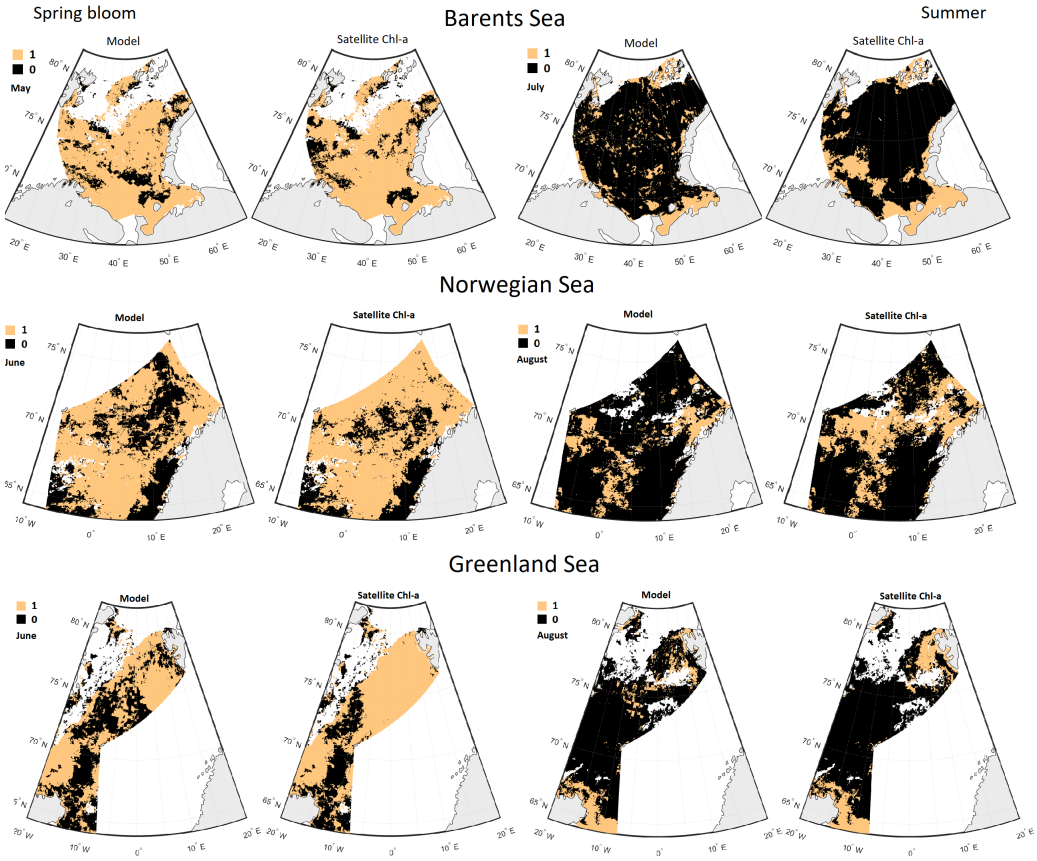

Figure 5. Validation results for the proposed models. Comparison of the estimated and remotely sensed position of high-productivity zones during a spring bloom and summer less productive months in 2019. Here "1" is a high-productivity zone with chlorophyll-*a* concentration greater than 1 mg m^{-3}, "0" is a low-productivity zone with chlorophyll-*a* concentration less than 1 mg m^{-3}. In each month, the left map refers to modeled results and the right map – to satellite data (test set).

bloom, Chl-*a* is dependent on MLD (i.e., a pycnocline needs to become shallower for the onset of a bloom). At the same time, correlation between the parameters is positive in summer: a decrease in MLD indicates stronger stratification, which prevents inflow of nutrients from the lower layers, thus, Chl-*a* decreases. In autumn, correlation is positive in areas where MLD is deepened, and vertical mixing occurs further: with deepening of MLD, nutrients can enter the surface layer, and Chl-*a* can increase.

4.2. Phytoplankton as the Main Suspended Matter in the Open Ocean

According to the results of our study, the relationship between Chl-*a* and Zeu is predominantly negative (r : $-0.9\ldots-0.7$), as has already been found in previous studies [*Delafontaine and Peters*, 1986; *Estrada et al.*, 1993; *Smith and Baker*, 1978].

This relationship is explained by several processes: firstly, during a bloom phytoplankton tends to shade itself (self-shading effect) [*Shigesada and Okubo*, 1981]. That in turn leads to a decrease of productivity in spring, when water turbidity increases due to abundant phytoplankton blooms (Zeu is shallow at this moment). Secondly, in summer, when Chl-*a* decreases due to nutrient limitation, Zeu increases since a decrease in dissolved and suspended matter allows light to penetrate into deeper layers. In autumn, two factors work together: a decrease in Zeu due to a decrease in surface illumination, and a decrease in Zeu due to an increase in the concentration of suspended matter (here once again suspended matter is mainly phytoplankton starting its autumn bloom).

4.3. Influence of Environmental Factors on Chlorophyll-a Concentration and the Formation of Highly Productive Zones

In this study we analyzed the correlation between Chl-*a* and environmental factors that affect phytoplankton's ability to photosynthesize and grow.

We found significant correlation between Chl-*a* and SST, Chl-*a* and PAR.

The nature of the relationship between Chl-*a* and SST can be explained by the seasonal variability of these parameters. In spring and early summer, when SST increases, a phytoplankton bloom begins and Chl-*a* rises. However, that is not always the case: in the northernmost parts of EAC a spring bloom does not occur, as the abundant ice-cover and light-limitation prevent phytoplankton growth until early summer [*Qu and Gabric*, 2022; *Silva et al.*, 2021]. Furthermore, in coastal regions the correlation is mostly inverse: warmer waters in the Norwegian shelf have been found to have a negative correlation with the onset of a spring bloom [*Hansen et al.*, 2010].

In summer, SST continues to increase, however, stratification is established, and phytoplankton stop actively growing, hence, the relationship is reversed. The positive correlation between Chl-*a* and SST in summer can be explained by abundant continental waters runoff. In this case, SST is an indicator of the influx of warm, nutrient-rich water from rivers or warm Atlantic waters, which cause a slight destruction of stratification, an influx of nutrients to the surface layer [*Ardyna and Arrigo*, 2020; *Qu and Liu*, 2020]. Additionally, positive correlation in the high latitudes could indicate a summer bloom that occurs in polar regions [*Silva et al.*, 2021].

Finally, in autumn, SST decreases, and Chl-*a* can increase again, due to the destruction of stratification, and upwelling of nutrients from underlying layers [*Ardyna and Arrigo*, 2020; *Dalpadado et al.*, 2020]. Alternatively, together with decreasing of SST, there is decreasing of Chl-*a* due to reducing phytoplankton photosynthetic activity.

Overall, we believe that remotely-sensed SST is more so an indicator of the variability of Chl-*a*, and less so a parameter that directly determines Chl-*a* in the area.

The correlation between Chl-*a* and PAR is determined both by the dependence of photosynthesis on light during bloom seasons – spring and autumn, – and by the parallel seasonal evolution of Chl-*a* and PAR during the summer season, when photosynthesis is less intense. During a spring bloom, the relationship between the parameters is positive: photosynthesis starts rapidly with a rise in light availability, and thus, Chl-*a* rises. Similar conditions have been described for the Barents and Greenland Seas in [*Qu and Gabric*, 2022], for the EAC – in [*Silva et al.*, 2021].

In summer, as light intensity decreases after the solstice, the maximum rate of photosynthesis decreases as well. Meanwhile, Chl-*a* decreases due to nutrient limitation, as strong stratification is established [*Ardyna and Arrigo*, 2020]. Moreover, at this time the waters are mostly dominated by coccolithophores, not diatoms and small flagellates, and they cannot be observed via Chl-*a* ocean color images [*Qu and Gabric*, 2022; *Silva et al.*, 2021]. Overall, correlation between the parameters is mostly positive, however we believe that at this time light availability is not the driving factor for the changes in monthly Chl-*a*.

Finally, in autumn, the relationship is mostly negative, since Chl-*a* increases with destruction of stratification through wind and convective mixing and the following nutrient influx, while PAR continues to decrease [*Silva et al.*, 2021].

We found some significant correlation between Chl-*a* and SSS, Chl-*a* and MLD.

The correlation between Chl-*a* and SSS almost always illustrates salinity as either an indicator of the intrusion of salty Atlantic waters into the region or an influx of fresh continental or glacial waters: in the first case, the relationship is positive, in the second, it is negative. The salty and dynamically active Atlantic waters mix the water column, destroying stratification; additional nutrients upwell from underlying layers and contribute to the increase of Chl-*a* [*Ardyna and Arrigo*, 2020]. Fresh water is an indicator of continental runoff (in summer and autumn), sufficient amount of nutrients is essential for diatoms blooming (mainly nitrates and silicates), as well as melting of the sea ice contributing to the phytoplankton bloom in a thin, well-lit fresh water layer that forms consequently in spring [*Perrette et al.*, 2011; *Silva et al.*, 2021].

Through analyzing the correlation between Chl-*a* and MLD, which is the most spatially universal in spring, a complex connection between Chl-*a* and the euphotic and upper mixed layers can be observed. In spring, as stratification is established, MLD becomes shallower and, after some time, coincides with the euphotic depth; phytoplankton, having "settled" on the pycnocline, begin to photosynthesize, when a sufficient amount of solar radiation and nutrients (accumulated during winter months) is reached. This relationship between the shallowing of ML and increase in Chl-*a* has been observed in the Labrador and Irminger Seas in the North Atlantic [*Naustvoll et al.*, 2020].

To further enhance our understanding of the conditions that influence Chl-*a* in each sea, we produced hexagonal binning plots (Figure 6) that show two of the most prevalent factors influencing productivity for each sea and their relationship to Chl-*a*: for the Barents and Greenland Seas SSS and PAR are the more important factors, while for the Norwegian Sea – SST and PAR take the lead.

In the Greenland and Norwegian Seas just before the start of the spring bloom, when phytoplankton are still limited by light, a thin layer above the shallow pycnocline can form due to the relatively fresh waters that come from glaciers melting on land as well as from sea ice melting [*Levasseur*, 2013]. This layer is relatively fresh and warm; it lies very close to the surface, so phytoplankton can comfortably photosynthesize in it even during limited light conditions [*Borstad and Gower*, 1984; *Tremblay and Gagnon*, 2009]. Moreover, mainland meltwater is rich in nutrients that are necessary for the growth of phytoplankton. These are, for example, silica compounds, which are the base for the diatom skeleton [*Anderson*, 1986; *Hegseth and Sundfjord*, 2008; *Perrette et al.*, 2011]. [*Oliver et al.*, 2018] modeled the same conditions for the Labrador Sea, confirming the increase in PP when glacial Greenland water flowed into the sea.

Furthermore, melt ponds that form on sea ice can provide phytoplankton with conditions that could lead to an increase in productivity due to the nutrients dissolved in the meltwater and abundant light comfortably penetrating the shallow ponds [*Chandler et al.*, 2015]. Under-ice blooms have also been detected in the Arctic containing high diatom concentrations that exhibited high growth and production rates [*Arrigo et al.*, 2012]. Conditions indicating such blooms are seen in Figure 6 in areas where PAR is between 10–20 E m^2 day^{-1}, salinity is below 33 psu, and SST is above 6 °C. Similar conditions were also observed at the end of June 2021 during the 83rd cruise of the RV "Academic Mstislav Keldysh" in the Kara Sea [*Demidov et al.*, 2022] at stations where ice melted within a month from the measurements taken.

During summer, photosynthesis is limited by nutrients. Thus, in spite of high illumination, there are low Chl-*a* values corresponding to data points with relatively high PAR, SST and salinity (Figure 6).

Local phytoplankton blooms are observed during the intrusion of dynamically active, nutrient-rich and salty Atlantic Ocean waters into the area [*Haug et al.*, 2017; *Torres-Valdés et al.*, 2013]. Similar conditions happen after vertical water mixing in the deep convection regions and in the frontal zones of the Greenland and Norwegian Seas (high illumination, high salinity and low temperature zones in Figure 6). For example, [*Hansen et al.*, 2010] described an increase in PP in anticyclonic eddies observed near the Norwegian Sea fronts. Vertical mixing can cause an upwelling of nutrients into the surface layer, which are then utilized by phytoplankton for photosynthesis.

In autumn, when illumination decreases again and salinity is relatively high, the second bloom can occur due to the beginning of winter convection. This is especially relevant for the Barents Sea (see Figure 6): high Chl-*a* is characteristic for the light-limited areas (PAR is about 20–30 E m^2 day^{-1}) with salinity above 30 psu. It is important to mention that high Chl-*a* coinciding with low PAR could be caused by errors in ocean color data characteristic of low-light conditions beyond 70°N, however most of these errors tend to be flagged as such at the L3 processing stage for MODIS and SeaWiFS sensors, whose data was used in this study [*Babin et al.*, 2015]. Conversely, some studies described conditions in the North Sea where under low-light conditions satellite sensors have failed to accurately detect the exact date of the onset of a bloom [*Silva et al.*, 2021].

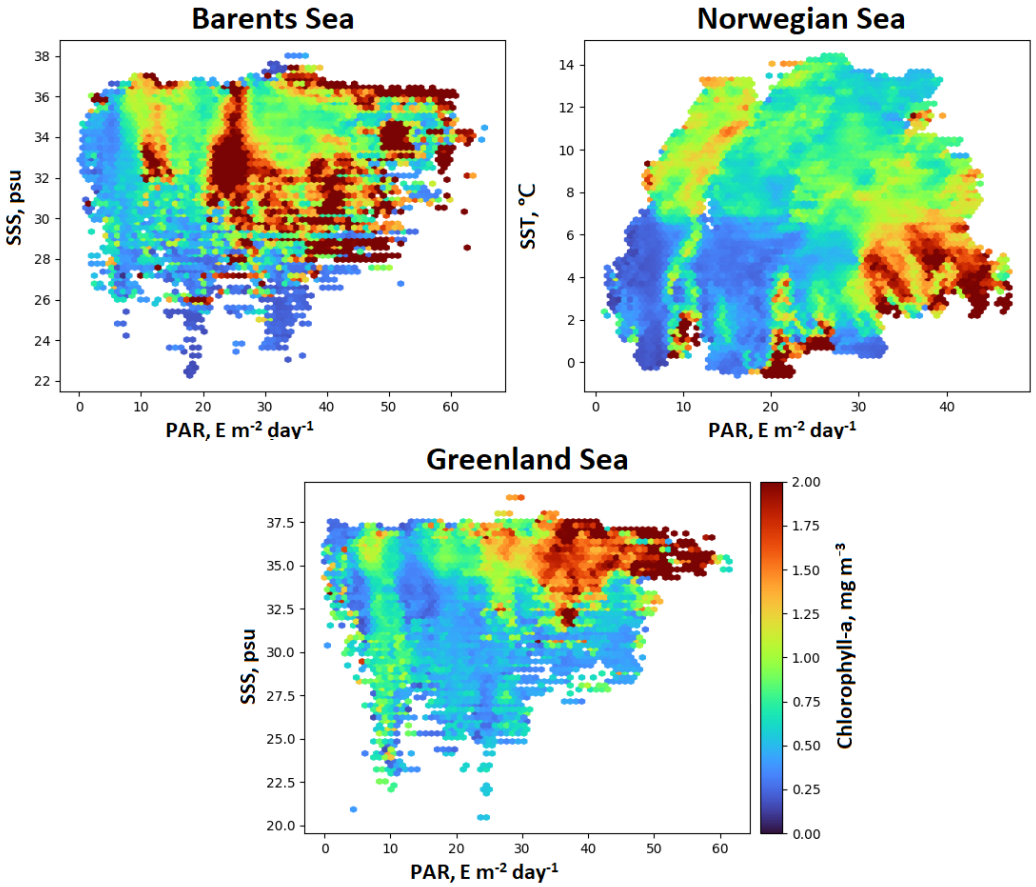

Figure 6. Hexagonal binning plots for the Barents, Norwegian and Greenland Seas: chlorophyll-*a* concentration (in color, mg m^{-3}) and environmental parameters: sea surface salinity (SSS, psu), sea surface temperature (SST, °C) and photosynthetically active radiation (PAR, E m^2 day^{-1}) in 2010–2019. Figure adapted from [*Kuzmina et al.*, 2023].

4.4. Models' Performance and its Affecting Factors

There are many models predicting the productivity of the Arctic seas, especially the European Arctic Corridor seas. Previous studies [*Martyanov et al.*, 2018; *Wassmann et al.*, 2006] have used physically–biologically coupled 3D modeling to predict PP and carbon flux in the Barents Sea; this model underestimated the vertical carbon export of the sea and, similarly to our models, had higher variability of results in the more ice-covered areas of the region. Another study found that PP in the region was influenced by nutrient availability, ice coverage and temperature- and wind-induced stratification [*Mousing et al.*, 2023]. A recent study of PP in the Greenland shelf has found that sea ice coverage was better seen and felt in models that used ocean color data as compared to models that used coupled 3D modeling [*Vernet et al.*, 2021].

Ocean productivity in this region is influenced by warm Atlantic waters and cold Arctic waters, as well as river and ice runoff, light availability and sea ice extent [*Mousing et al.*, 2023]. Our results showed greater variability of model performance (assessed through MQMs and quantitively through the sum-total area of HPZs in 2019) during spring, when the productivity is more influenced by sea ice extent [*Mousing et al.*, 2023; *Wassmann et al.*, 2006]. We did not use ice extent or sea ice concentration data in our models, so perhaps part of the variability and bias of our models could be explained by this. This could be further investigated in future projects.

5. Conclusions

In this study we describe the spatial and temporal distribution of the connections between Chl-*a* and environmental parameters in the EAC. We confirmed that Chl-*a* is greatly dependent on light availability: the best correlation is noted between Chl-*a* and PAR, and it is predominantly positive. The relationship between Chl-*a* and SST is positive in spring, but almost strictly negative in summer. A somewhat weaker relationship is seen between Chl-*a* and SSS, it is positive in spring. The relationship between Chl-*a* and MLD is strictly negative in spring and mostly positive in summer.

According to the results of our modeling, the greatest contribution to the variability of Chl-*a* is made by the variability of PAR (contribution – 28–32%), SSS (26–31%) and SST (25–29%), the contribution of MLD is almost twice as low (12–17%). Together, these parameters describe the conditions that most favorably affect the productivity of the area: the availability of light in the spring and autumn periods and the availability of nutrients with vertical mixing in the summer and autumn periods.

Modeling the position of high- and low-productivity zones (HPZ and LPZ, respectively) in the studied seas showed that: 1) all three models predict the overall temporal and spatial variability of the distribution of HPZs and LPZs with an accuracy comparable to observed values (depending on the sample, 66 to 96% of the results were correct); 2) the model for the Greenland Sea has the best overall performance, since it showed the highest quality metrics and almost always correctly predicted both the total area and the location of HPZs; 3) the model for the Norwegian Sea on the whole correctly determines the position of HPZs, but underestimates their total area; 4) the model for the Barents Sea does not always correctly predict the position of HPZs, but it is the best at predicting the total area of HPZs. The models' performance might in the future be improved by introducing more factors (sea ice concentration and thickness, wind stress).

Acknowledgments. The authors acknowledge Saint Petersburg State University for a research project no. 116442164.

Appendix A

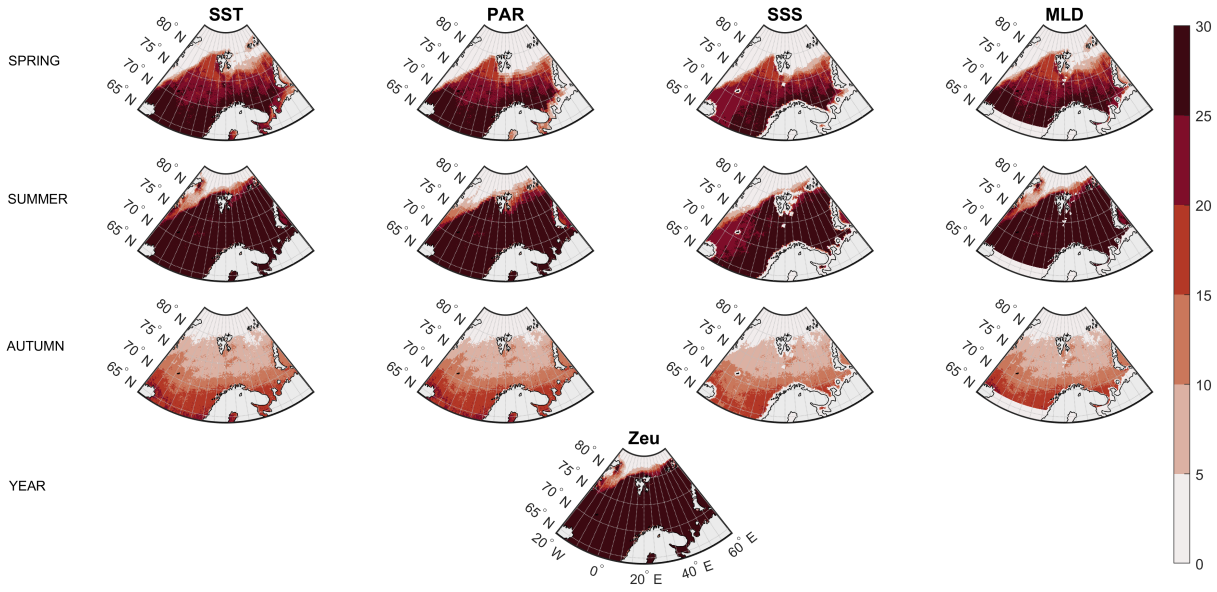

Figure A1. Size of dataset (N) used to calculate correlation coefficients between chlorophyll-*a* concentration (Chl-*a*, mg m^{-3}) and environmental parameters: sea surface temperature (SST, °C), photosynthetically active radiation (PAR, E m^2 day^{-1}), sea surface salinity (SSS, psu), mixed layer depth (MLD, m) and euphotic layer depth (Zeu, m) in 2010–2019.

References

Anderson, G. F. (1986), Silica, diatoms and a freshwater productivity maximum in Atlantic Coastal Plain estuaries, Chesapeake Bay, *Estuarine, Coastal and Shelf Science*, *22*(2), 183–197, https://doi.org/10.1016/0272-7714(86)90112-5.

Ardyna, M., and K. R. Arrigo (2020), Phytoplankton dynamics in a changing Arctic Ocean, *Nature Climate Change*, *10*(10), 892–903, https://doi.org/10.1038/s41558-020-0905-y.

Ardyna, M., M. Babin, M. Gosselin, et al. (2014), Recent arctic ocean sea ice loss triggers novel fall phytoplankton blooms, *Geophysical Research Letters*, *41*(17), 6207–6212, https://doi.org/10.1002/2014gl061047.

Arrigo, K. R., and G. L. van Dijken (2015), Continued increases in Arctic Ocean primary production, *Progress in Oceanography*, *136*, 60–70, https://doi.org/10.1016/j.pocean.2015.05.002.

Arrigo, K. R., D. K. Perovich, R. S. Pickart, et al. (2012), Massive Phytoplankton Blooms Under Arctic Sea Ice, *Science*, *336*(6087), 1408–1408, https://doi.org/10.1126/science.1215065.

Babin, M., K. Arrigo, S. Bélanger, and M.-H. Forget (Eds.) (2015), *Ocean Colour Remote Sensing in Polar Seas*, IOCCG Report Series, No. 16, International Ocean Colour Coordinating Group, Dartmouth, Canada.

Balch, W. (1992), The remote sensing of ocean primary productivity: Use of a new data compilation to test satellite algorithms, *Journal of Geophysical Research: Oceans*, *97*(C3), 3689–3689, https://doi.org/10.1029/92jc00372.

Balch, W. M., P. M. Holligan, S. G. Ackleson, and K. J. Voss (1991), Biological and optical properties of mesoscale coccolithophore blooms in the Gulf of Maine, *Limnology and Oceanography*, *36*(4), 629–643, https://doi.org/10.4319/lo.1991.36.4.0629.

Bashmachnikov, I. L., A. M. Fedorov, A. V. Vesman, et al. (2018), Thermohaline convection in the subpolar seas of the North Atlantic from satellite and in situ observations. Part 1: localization of the deep convection sites, *Sovremennye problemy distantsionnogo zondirovaniya Zemli iz kosmosa*, *15*(7), 184–194, https://doi.org/10.21046/2070-7401-2018-15-7-184-194 (in Russian).

Behrenfeld, M. J. (2010), Abandoning Sverdrup's Critical Depth Hypothesis on phytoplankton blooms, *Ecology*, *91*(4), 977–989, https://doi.org/10.1890/09-1207.1.

Behrenfeld, M. J., and P. G. Falkowski (1997), Photosynthetic rates derived from satellite-based chlorophyll concentration, *Limnology and Oceanography*, *42*(1), 1–20, https://doi.org/10.4319/lo.1997.42.1.0001.

Behrenfeld, M. J., E. Boss, D. A. Siegel, and D. M. Shea (2005), Carbon-based ocean productivity and phytoplankton physiology from space, *Global Biogeochemical Cycles*, *19*(1), https://doi.org/10.1029/2004GB002299.

Bode, A., J. Hare, W. K. W. Li, et al. (2011), Chlorophyll and primary production in the North Atlantic, in *ICES Status Report on Climate Change in the North Atlantic*, pp. 77–102, International Council for the Exploration of the Sea, Denmark.

Børsheim, K. Y., S. Milutinović, and K. F. Drinkwater (2014), TOC and satellite-sensed chlorophyll and primary production at the Arctic Front in the Nordic Seas, *Journal of Marine Systems*, *139*, 373–382, https://doi.org/10.1016/j.jmarsys.2014.07.012.

Borstad, G. A., and J. F. R. Gower (1984), Phytoplankton Chlorophyll Distribution in the Eastern Canadian Arctic, *ARCTIC*, *37*(3), https://doi.org/10.14430/arctic2195.

Brody, S. R., and M. S. Lozier (2015), Characterizing upper-ocean mixing and its effect on the spring phytoplankton bloom with in situ data, *ICES Journal of Marine Science*, *72*(6), 1961–1970, https://doi.org/10.1093/icesjms/fsv006.

Carr, M.-E. (2001), Estimation of potential productivity in Eastern Boundary Currents using remote sensing, *Deep Sea Research Part II: Topical Studies in Oceanography*, *49*(1–3), 59–80, https://doi.org/10.1016/s0967-0645(01)00094-7.

Carr, M.-E., M. A. M. Friedrichs, M. Schmeltz, et al. (2006), A comparison of global estimates of marine primary production from ocean color, *Deep Sea Research Part II: Topical Studies in Oceanography*, *53*(5–7), 741–770, https://doi.org/10.1016/j.dsr2.2006.01.028.

Cazzaniga, I., G. Zibordi, and F. Mélin (2021), Spectral variations of the remote sensing reflectance during coccolithophore blooms in the Western Black Sea, *Remote Sensing of Environment*, *264*, 112,607, https://doi.org/10.1016/j.rse.2021.112607.

Chandler, D. M., J. D. Alcock, J. L. Wadham, et al. (2015), Seasonal changes of ice surface characteristics and productivity in the ablation zone of the Greenland Ice Sheet, *The Cryosphere*, *9*(2), 487–504, https://doi.org/10.5194/tc-9-487-2015.

Chiswell, S. M. (2011), Annual cycles and spring blooms in phytoplankton: don't abandon Sverdrup completely, *Marine Ecology Progress Series*, *443*, 39–50, https://doi.org/10.3354/meps09453.

Cutler, D. R., T. C. Edwards, K. H. Beard, et al. (2007), Random Forests for Classification in Ecology, *Ecology*, *88*(11), 2783–2792, https://doi.org/10.1890/07-0539.1.

Dalpadado, P., K. R. Arrigo, G. L. van Dijken, et al. (2020), Climate effects on temporal and spatial dynamics of phytoplankton and zooplankton in the Barents Sea, *Progress in Oceanography*, *185*, 102,320, https://doi.org/10.1016/j.pocean.2020.102320.

Delafontaine, Y., and R. Peters (1986), Empirical relationship for marine primary production - the effect of environmental variables, *Oceanologica Acta*, *9*, 65–72.

Demidov, A. B., V. M. Sergeeva, V. I. Gagarin, et al. (2022), Size-Fractionated Primary Production and Chlorophyll in the Kara Sea during the First-Year Ice Retreat, *Oceanology*, *62*(3), 346–357, https://doi.org/10.1134/s0001437022030031.

Estrada, M., C. Marrasé, M. Latasa, et al. (1993), Variability of deep chlorophyll maximum characteristics in the Northwestern Mediterranean, *Marine Ecology Progress Series*, *92*, 289–300, https://doi.org/10.3354/meps092289.

Falkowski, P. G., R. T. Barber, and V. Smetacek (1998), Biogeochemical Controls and Feedbacks on Ocean Primary Production, *Science*, *281*(5374), 200–206, https://doi.org/10.1126/science.281.5374.200.

Fischer, A., E. Moberg, H. Alexander, et al. (2014), Sixty Years of Sverdrup: A Retrospective of Progress in the Study of Phytoplankton Blooms, *Oceanography*, *27*(1), 222–235, https://doi.org/10.5670/oceanog.2014.26.

Hansen, B., U. C. Berggreen, K. S. Tande, and H. C. Eilertsen (1990), Post-bloom grazing by Calanus glacialis, C. finmarchicus and C. hyperboreus in the region of the Polar Front, Barents Sea, *Marine Biology*, *104*(1), 5–14, https://doi.org/10.1007/bf01313151.

Hansen, C., E. Kvaleberg, and A. Samuelsen (2010), Anticyclonic eddies in the Norwegian Sea; their generation, evolution and impact on primary production, *Deep Sea Research Part I: Oceanographic Research Papers*, *57*(9), 1079–1091, https://doi.org/10.1016/j.dsr.2010.05.013.

Haug, T., B. Bogstad, M. Chierici, et al. (2017), Future harvest of living resources in the Arctic Ocean north of the Nordic and Barents Seas: A review of possibilities and constraints, *Fisheries Research*, *188*, 38–57, https://doi.org/10.1016/j.fishres.2016.12.002.

Hegseth, E. N., and A. Sundfjord (2008), Intrusion and blooming of Atlantic phytoplankton species in the high Arctic, *Journal of Marine Systems*, *74*(1–2), 108–119, https://doi.org/10.1016/j.jmarsys.2007.11.011.

Joseph, V. R. (2022), Optimal ratio for data splitting, *Statistical Analysis and Data Mining: The ASA Data Science Journal*, *15*(4), 531–538, https://doi.org/10.1002/sam.11583.

Kahru, M., V. Brotas, M. Manzano-Sarabia, and B. G. Mitchell (2011), Are phytoplankton blooms occurring earlier in the Arctic?: PHYTOPLANKTON BLOOMS IN THE ARCTIC, *Global Change Biology*, *17*(4), 1733–1739, https://doi.org/10.1111/j.1365-2486.2010.02312.x.

Kondrik, D., D. Pozdnyakov, and L. Pettersson (2017), Tendencies in Coccolithophorid Blooms in Some Marine Environments of the Northern Hemisphere according to the Data of Satellite Observations in 1998-2013, *Izvestiya, Atmospheric and Oceanic Physics*, *53*(9), 955–964, https://doi.org/10.1134/s000143381709016x.

Kuzmina, S., P. Lobanova, and I. Bashmachnikov (2022), Spatial and temporal variability of chlorophyll-a and its relation to physical and biological parameters: a case study for the European Arctic Corridor, in *PICES-2022 Book Abstracts*, p. 127, PICES Secretariat, Busan, Korea.

Kuzmina, S., P. Lobanova, and S. Chepikova (2023), Modeling Chlorophyll a Concentration for the European Arctic Corridor Based on Environmental Parameters, in *Complex Investigation of the World Ocean (CIWO-2023)*, pp. 456–462, Springer Nature Switzerland, https://doi.org/10.1007/978-3-031-47851-2_55.

Lee, Y. J., P. A. Matrai, M. A. M. Friedrichs, et al. (2015a), An assessment of phytoplankton primary productivity in the Arctic Ocean from satellite ocean color/in situ chlorophyll-a based models, *Journal of Geophysical Research: Oceans*, *120*(9), 6508–6541, https://doi.org/10.1002/2015jc011018.

Lee, Z., J. Marra, M. J. Perry, and M. Kahru (2015b), Estimating oceanic primary productivity from ocean color remote sensing: A strategic assessment, *Journal of Marine Systems*, *149*, 50–59, https://doi.org/10.1016/j.jmarsys.2014.11.015.

Levasseur, M. (2013), Impact of Arctic meltdown on the microbial cycling of sulphur, *Nature Geoscience*, *6*(9), 691–700, https://doi.org/10.1038/ngeo1910.

Lewandowska, A. M., M. Striebel, U. Feudel, et al. (2015), The importance of phytoplankton trait variability in spring bloom formation, *ICES Journal of Marine Science*, *72*(6), 1908–1915, https://doi.org/10.1093/icesjms/fsv059.

Lewis, K. M., G. L. van Dijken, and K. R. Arrigo (2020), Changes in phytoplankton concentration now drive increased Arctic Ocean primary production, *Science*, *369*(6500), 198–202, https://doi.org/10.1126/science.aay8380.

Lobanova, P. V. (2017), Satellite Derived Algorithms of Primary Production Assessment in Waters With Various Oceanographic Conditions: Case Studies of the Northeast Atlantic and the Japan/East Sea, candthesis, Saint Petersburg State University, Saint Petersburg (in Russian).

Longhurst, A. R. (2007), *Ecological geography of the sea*, ii ed., Elsevier, Amsterdam; Boston, MA, https://doi.org/10.1016/b978-0-12-455521-1.x5000-1.

Makarevich, P., V. Vodopianova, and A. Bulavina (2022), Dynamics of the Spatial Chlorophyll-A Distribution at the Polar Front in the Marginal Ice Zone of the Barents Sea during Spring, *Water*, *14*(1), 101, https://doi.org/10.3390/w14010101.

Martyanov, S. D., A. Y. Dvornikov, V. A. Ryabchenko, et al. (2018), Investigation of the relationship between primary production and sea ice in the Arctic seas: Assessments based on a small-component model of marine ecosystem, *Fundamentalnaya i Prikladnaya Gidrofizika*, *11*(2), 108–117, https://doi.org/10.7868/S2073667318020107.

Morel, A. (1978), Available, usable, and stored radiant energy in relation to marine photosynthesis, *Deep Sea Research*, *25*(8), 673–688, https://doi.org/10.1016/0146-6291(78)90623-9.

Morel, A., and L. Prieur (1977), Analysis of variations in ocean color, *Limnology and Oceanography*, *22*(4), 709–722, https://doi.org/10.4319/lo.1977.22.4.0709.

Mousing, E. A., I. Ellingen, S. S. Hjøllo, et al. (2023), Why do regional biogeochemical models produce contrasting future projections of primary production in the Barents Sea?, *Journal of Sea Research*, *192*, 102,366, https://doi.org/10.1016/j.seares.2023.102366.

Naustvoll, L. J., W. Melle, T. Klevjer, et al. (2020), Dynamics of phytoplankton species composition, biomass and nutrients in the North Atlantic during spring and summer - A trans-Atlantic study, *Deep Sea Research Part II: Topical Studies in Oceanography*, *180*, 104,890, https://doi.org/10.1016/j.dsr2.2020.104890.

Nguyen, Q. H., H.-B. Ly, L. S. Ho, et al. (2021), Influence of Data Splitting on Performance of Machine Learning Models in Prediction of Shear Strength of Soil, *Mathematical Problems in Engineering*, *2021*, 1–15, https://doi.org/10.1155/2021/4832864.

Nielsen, E. S. (1963), Productivity, definition and measurement, in *The Sea. Volume 2*, pp. 129–164, Wiley, New York.

Odum, E. P. (1971), *Fundamentals of Ecology*, third ed., 574 pp., W. B. Saunders Co., Philadelphia.

Oliver, H., H. Luo, R. M. Castelao, et al. (2018), Exploring the Potential Impact of Greenland Meltwater on Stratification, Photosynthetically Active Radiation, and Primary Production in the Labrador Sea, *Journal of Geophysical Research: Oceans*, *123*(4), 2570–2591, https://doi.org/10.1002/2018jc013802.

Oziel, L., A. Baudena, M. Ardyna, et al. (2020), Faster Atlantic currents drive poleward expansion of temperate phytoplankton in the Arctic Ocean, *Nature Communications*, *11*(1), https://doi.org/10.1038/s41467-020-15485-5.

Oziel, L., P. Massicotte, M. Babin, and E. Devred (2022), Decadal changes in Arctic Ocean Chlorophyll a: Bridging ocean color observations from the 1980s to present time, *Remote Sensing of Environment*, *275*, 113,020, https://doi.org/10.1016/j.rse.2022.113020.

Perrette, M., A. Yool, G. D. Quartly, and E. E. Popova (2011), Near-ubiquity of ice-edge blooms in the Arctic, *Biogeosciences*, *8*(2), 515–524, https://doi.org/10.5194/bg-8-515-2011.

Platt, T., and S. Sathyendranath (1988), Oceanic Primary Production: Estimation by Remote Sensing at Local and Regional Scales, *Science*, *241*(4873), 1613–1620, https://doi.org/10.1126/science.241.4873.1613.

Qu, B., and A. J. Gabric (2022), The multi-year comparisons of chlorophyll and sea ice in Greenland Sea and Barents Sea and their relationships with the North Atlantic Oscillation, *Journal of Marine Systems*, *231*, 103,749, https://doi.org/10.1016/j.jmarsys.2022.103749.

Qu, B., and X. Liu (2020), The effect of wind and temperature to phytoplankton biomass during blooming season in Barents Sea, *Dynamics of Atmospheres and Oceans*, *91*, 101,157, https://doi.org/10.1016/j.dynatmoce.2020.101157.

Reigstad, M., P. Wassmann, C. Wexels Riser, et al. (2002), Variations in hydrography, nutrients and chlorophyll a in the marginal ice-zone and the central Barents Sea, *Journal of Marine Systems*, *38*(1–2), 9–29, https://doi.org/10.1016/s0924-7963(02)00167-7.

Riley, G. A. (1940), Limnological Studies in Connecticut. Part III. The Plankton of Linsley Pond, *Ecological Monographs*, *10*(2), 279–306, https://doi.org/10.2307/1948608.

Rivero-Calle, S., A. Gnanadesikan, C. E. D. Castillo, et al. (2015), Multidecadal increase in North Atlantic coccolithophores and the potential role of rising CO_2, *Science*, *350*(6267), 1533–1537, https://doi.org/10.1126/science.aaa8026.

Ryther, J. H., and C. S. Yentsch (1957), The Estimation of Phytoplankton Production in the Ocean from Chlorophyll and Light Data, *Limnology and Oceanography*, *2*(3), 281–286, https://doi.org/10.1002/lno.1957.2.3.0281.

Sakshaug, E., G. H. Johnsen, and K. M. Kovacs (Eds.) (2009), *Ecosystem Barents Sea*, 587 pp., Tapir Academic Press, Trondheim.

Sathyendranath, S., R. Ji, and H. Browman (2015), Revisiting Sverdrup's critical depth hypothesis, *ICES Journal of Marine Science*, *72*(6), 1892–1896, https://doi.org/10.1093/icesjms/fsv110.

Shigesada, N., and A. Okubo (1981), Analysis of the self-shading effect on algal vertical distribution in natural waters, *Journal of Mathematical Biology*, *12*(3), 311–326, https://doi.org/10.1007/bf00276919.

Siegel, D. A., S. C. Doney, and J. A. Yoder (2002), The North Atlantic Spring Phytoplankton Bloom and Sverdrup's Critical Depth Hypothesis, *Science*, *296*(5568), 730–733, https://doi.org/10.1126/science.1069174.

Silva, E., F. Counillon, J. Brajard, et al. (2021), Twenty-One Years of Phytoplankton Bloom Phenology in the Barents, Norwegian, and North Seas, *Frontiers in Marine Science*, *8*, https://doi.org/10.3389/fmars.2021.746327.

Skogen, M. D., E. Svendsen, J. Berntsen, et al. (1995), Modelling the primary production in the North Sea using a coupled three-dimensional physical-chemical-biological ocean model, *Estuarine, Coastal and Shelf Science*, *41*(5), 545–565, https://doi.org/10.1016/0272-7714(95)90026-8.

Slagstad, D., and K. Støle-Hansen (1991), Dynamics of plankton growth in the Barents Sea: model studies, *Polar Research*, *10*(1), 173–186, https://doi.org/10.3402/polar.v10i1.6736.

Smith, R. C., and K. S. Baker (1978), The bio-optical state of ocean waters and remote sensing, *Limnology and Oceanography*, *23*(2), 247–259, https://doi.org/10.4319/lo.1978.23.2.0247.

Sverdrup, H. U. (1953), On Conditions for the Vernal Blooming of Phytoplankton, *ICES Journal of Marine Science*, *18*(3), 287–295, https://doi.org/10.1093/icesjms/18.3.287.

Talling, J. F. (1957), Photosynthetic Characteristics of Some Freshwater Plankton Diatoms in Relation to Underwater Radiation, *New Phytologist*, *56*(1), 29–50, https://doi.org/10.1111/j.1469-8137.1957.tb07447.x.

Teira, E., B. M. no, E. M. nón, et al. (2005), Variability of chlorophyll and primary production in the Eastern North Atlantic Subtropical Gyre: potential factors affecting phytoplankton activity, *Deep Sea Research Part I: Oceanographic Research Papers*, *52*(4), 569–588, https://doi.org/10.1016/j.dsr.2004.11.007.

Torres-Valdés, S., T. Tsubouchi, S. Bacon, et al. (2013), Export of nutrients from the Arctic Ocean, *Journal of Geophysical Research: Oceans*, *118*(4), 1625–1644, https://doi.org/10.1002/jgrc.20063.

Tremblay, J.-E., and J. Gagnon (2009), The effects of irradiance and nutrient supply on the productivity of Arctic waters: a perspective on climate change, in *Influence of Climate Change on the Changing Arctic and Sub-Arctic Conditions*, pp. 73–93, Springer Netherlands, https://doi.org/10.1007/978-1-4020-9460-6_7.

Vernet, M., I. Ellingsen, C. Marchese, et al. (2021), Spatial variability in rates of net primary production (NPP) and onset of the spring bloom in Greenland shelf waters, *Progress in Oceanography*, *198*, 102,655, https://doi.org/10.1016/j.pocean.2021.102655.

Wassmann, P., D. Slagstad, C. W. Riser, and M. Reigstad (2006), Modelling the ecosystem dynamics of the Barents Sea including the marginal ice zone, *Journal of Marine Systems*, *59*(1–2), 1–24, https://doi.org/10.1016/j.jmarsys.2005.05.006.

Wassmann, P., D. Slagstad, and I. Ellingsen (2010), Primary production and climatic variability in the European sector of the Arctic Ocean prior to 2007: preliminary results, *Polar Biology*, *33*(12), 1641–1650, https://doi.org/10.1007/s00300-010-0839-3.